



Sulfonated poly(ether ether ketone)-Protic ionic Liquid-Based anhydrous Proton-Conducting composite polymer electrolyte membranes for High-Temperature fuel cell applications

Arfat Anis^{a,*}, Manawwer Alam^b, Ravindra Kumar Gupta^c, Abdullah Alhamidi^a,
Hamid Shaikh^a, Anesh Manjaly Poulouse^a, Mohammad Asif Alam^d, Saeed M. Al-Zahrani^a

^a SABIC Polymer Research Center (SPRC), Chemical Engineering Department, King Saud University, Riyadh 11421, Saudi Arabia

^b Department of Chemistry, College of Science, King Saud University, Riyadh 11451, Saudi Arabia

^c King Abdullah Institute for Nanotechnology, King Saud University, Riyadh 11451, Saudi Arabia

^d Center of Excellence for Research in Engineering Materials (CEREM), King Saud University, Riyadh 11421, Saudi Arabia

ARTICLE INFO

Keywords:

Protic ionic liquids
Sulfonated poly(ether ether ketone)
Polymer electrolyte membrane
Thermal analysis
Anhydrous proton conductivity
Electrochemical impedance spectroscopy

ABSTRACT

A high-temperature polymer electrolyte membrane fuel cell (PEMFC) has enormous potential to produce clean energy with minimal environmental pollution along with high energy density and conversion efficiency. In the present work, anhydrous proton-conducting polymer electrolyte membranes for prospective high-temperature fuel cell application were successfully prepared using different protic ionic liquids (PILs) and sulfonated poly(ether ether ketone) (SPEEK). The protic ionic liquids (PILs), 2-hydroxyethylammonium formate, diethylmethyl ammonium triflate, 1-ethylimidazolium bis(trifluoromethylsulfonyl)imide, 1,2-dimethyl imidazolium bis(trifluoro methylsulfonyl)imide, and diethylmethylammonium methanesulfonate were selected based on their favorable physicochemical properties. The effect of the incorporation of the PIL on the structural, thermal, and electrical transport properties of the composite SPEEK polymer electrolyte membranes was studied. The prepared polymer electrolyte membranes (PEMs) were characterized using Fourier transform infrared (FTIR) spectroscopy, thermogravimetric analysis (TGA), differential scanning calorimetry (DSC), X-ray diffractometry (XRD), and electrochemical impedance spectroscopy (EIS) techniques. FTIR results indicated an interaction between the PIL and the SPEEK, which resulted in homogeneous and flexible membranes. The DSC results confirmed good miscibility and elucidated plasticizing effect of the incorporated PIL on the SPEEK polymer matrix. All the PEMs showed good thermal stability and high-temperature anhydrous proton conductivity, achieving best proton conductivity, $\approx 8 \times 10^{-3} \text{ S cm}^{-1}$ at 120 °C and low activation energy $\approx 0.26 \text{ eV}$, making it suitable for prospective high-temperature PEMFC applications.

1. Introduction

Ion-conducting polymers are of significant importance for applications in fuel cells, batteries, and supercapacitors. Proton conducting polymer electrolytes from amongst the various ion conducting polymers, have been extensively studied for their potential application in polymer electrolyte membrane fuel cells (PEMFC) (Zhang and Shen, 2012). PEMFC has enormous potential to produce clean energy with minimal environmental pollution along with high energy density and conversion efficiency. Presently the most commonly used polymer electrolyte membrane (PEM) is a perfluorosulfonic acid-based polymer electrolyte

membrane commercially known as Nafion (Devanathan, 2008). The proton conduction in Nafion is dependent on the hydration state of these membranes which limits the operating temperature of these membranes to around 80 °C, temperature beyond 80 °C leads to loss of hydration resulting in a drop in ionic conductivity of these membranes. PEMFCs which can operate at temperatures above 100 °C offer several important advantages such as simple heat and water management systems, improved reaction kinetics of the electrode materials, improved platinum catalyst tolerance to carbon monoxide poisoning, etc. (Johnson et al., 2012).

Developing polymer electrolyte membranes suitable for high

* Corresponding author.

E-mail address: arafat@ksu.edu.sa (A. Anis).

<https://doi.org/10.1016/j.jksus.2024.103215>

Received 10 February 2024; Received in revised form 27 March 2024; Accepted 14 April 2024

Available online 16 April 2024

1018-3647/© 2024 The Author(s). Published by Elsevier B.V. on behalf of King Saud University. This is an open access article under the CC BY-NC-ND license (<http://creativecommons.org/licenses/by-nc-nd/4.0/>).

temperature operations are highly desirable and has drawn immense attention. The polybenzimidazole (PBI) matrix impregnated with phosphoric acid stands out as one of the most recognized polymer electrolytes for high-temperature PEMFCs (Quartarone and Mustarelli, 2012). Nevertheless, phosphoric acid-doped PBI membranes demonstrate optimal proton conductivity typically at phosphoric acid loadings exceeding 5.0 acid molecules per PBI polymer repeat unit (Cappadonia et al., 1999). However, a significant drawback emerges from the auto-dehydration of phosphoric acid at higher temperatures presenting a notable limitation that is attributed to the formation of oligomers with lower conductivity (Eguizábal et al., 2013).

Sulfonated poly(ether ether ketone) (SPEEK), is an aromatic polymer and has been extensively studied as a high-performance, cost-effective polymer electrolyte membrane for commercial fuel cell applications. SPEEK and its composite membranes have demonstrated commendable performance in diverse applications like adsorption, pervaporation, gas separation, redox flow batteries, sensors, and actuators. SPEEK membranes have good thermal stability along with exceptional chemical and oxidative resistance which enables them to offer excellent service life.

The proton mobility and conductivity of SPEEK depend upon the degree of sulfonation, higher sulfonation enhances ionic conductivity but diminishes the mechanical strength due to higher water uptake characteristics of the resulting SPEEK. To address these shortcomings of hydration-dependent proton conductivity and subsequent deterioration in the mechanical properties of SPEEK we utilized protic ionic liquids (PIL) to fabricate SPEEK-based composite PEMs. SPEEK has been widely explored as the polymer matrix for incorporating protic ionic liquids, owing to its acceptable structural stability and the presence of abundant $-SO_3H$ aggregated ionic clusters (Wang et al., 2007).

The incorporation of the protic ionic liquids in the SPEEK polymer matrix aids proton mobility and hence augments the proton conductivity of the resulting composite PEMs without the need for any hydration. Hence, the resulting PEMs can be utilized under non-humid conditions and at higher temperatures well above 100 °C. Protic ionic liquids serve as a material of choice for the fabrication of a composite polymer electrolyte for PEMFCs owing to their properties, such as high chemical and thermal stability, low melting temperature and volatility, low toxicity, non-flammability, wide electrochemical stability range and good anhydrous proton conductivity at elevated temperatures.

Wang et al., 2017 investigated composite membranes of SPEEK with different ionic liquids and mesoporous silica and reported that the composite PEM with 50 wt% of 1-butyl-3-methylimidazolium tetrafluoroborate showed the highest anhydrous proton conductivity of $15 \times 10^{-3} \text{ S cm}^{-1}$ at 200 °C. Yilmazoglu et al., 2021 reported the dielectric behavior and proton conductivity of $5.45 \times 10^{-4} \text{ S cm}^{-1}$ for polymer electrolytes prepared by the incorporation of 1-ethyl-3-methylimidazolium tetrafluoroborate in SPEEK polymer matrix by solution casting method. Yilmazoglu et al. (2023) fabricated 1-ethyl-3-methylimidazolium tetrafluoroborate ionic liquid incorporated SPEEK/Chitosan composite polymer electrolytes and they obtained the maximum room temperature conductivity of $9.87 \times 10^{-3} \text{ S cm}^{-1}$ for the prepared composites and the conductivity decreased with increase in measurement temperature.

Maiti et al., 2023 reported the introduction of propyl sulfonic acid functionalized graphene oxide into SPEEK-sulfonated poly(benzimidazole) blend and demonstrated improvement in the thermal and chemical stability and mechanical properties of the composites along with good improvement in proton conductivity which reached around 0.17 S cm^{-1} at 90 °C but the values reported were at 100 % relative humidity conditions. Sun et al., 2023 reported fabrication of several different binary hybrid membranes through one-step encapsulation of different ionic liquids in SPEEK. They observed ILs doping improved the proton conductivity of the SPEEK membrane and obtained highest proton conductivity of $25 \times 10^{-3} \text{ S cm}^{-1}$ at 120 °C suitable for use in PEMFC at medium temperature. Xiong et al., 2024 fabricated composite membranes by electrostatic spinning, ionic liquid encapsulated

halloysite nanotube incorporated into SPEEK. They reported one dimensional ionogels, axially and uniformly aligned in the fiber direction with good water absorption, and the composite membranes showed improved proton conductivity which was humidity dependent and not reported for anhydrous conditions.

The most commonly used method for the fabrication of PIL-based composite membranes is by incorporating PIL into the polymer solution. In this approach, the PIL is either dissolved or dispersed within the polymer solution containing both the polymer and the solvent. The physicochemical features of the resulting composite membranes strongly depend on the compatibility between the PIL and the polymer as well as on their content ratio. In this work we selected different ammonium and imidazolium cation-based protic ionic liquids with proton conductivity in the mS range for the preparation of the SPEEK-PIL composite membranes for prospective high temperature PEMFC application. The structural, thermal, morphological and proton conducting properties of the composite membranes were evaluated and discussed in detail.

2. Materials and methods

2.1. Materials

Sulfonated poly(ether ether ketone) (SPEEK) FUMION® E-600 polymer fibers in K^+ form, IEC around 1.65 meq g^{-1} , was purchased from FumaTech-BWT GmbH, Bietigheim-Bissingen, Germany. Hydrochloric acid 37 % PA-ACS-ISO was purchased from Panreac, E.U. N-methylpyrrolidone (NMP) was purchased from Sigma Aldrich, USA. Protic ionic liquids, 2-hydroxyethylammonium formate, diethylmethylammonium triflate, 1-ethylimidazolium bis(trifluoromethylsulfonyl)imide, 1,2-dimethylimidazolium bis(trifluoromethylsulfonyl)imide, and diethylmethylammonium methanesulfonate were obtained from IoLiTec Ionic Liquids Technologies GmbH, Heilbronn, Germany. Table 1 lists the physicochemical properties of these PILs and their chemical structures are shown in Figure S1 (Supplementary Information). All chemicals were used as received without any further purification.

2.2. Methods

2.2.1. Polymer electrolyte membrane fabrication

The SPEEK fibers obtained were immersed overnight in 1 M HCl on a shaking plate for conditioning to ensure that all sulfonate groups had an H^+ as their counterion. Subsequently, the fibers were washed with demineralized water, refreshing the water multiple times until reaching a neutral pH, and then dried overnight in a vacuum oven at 80 °C. A solution containing 10 wt% SPEEK was prepared by dissolving SPEEK fibers in NMP, heated overnight at 120 °C with stirring. Pure SPEEK membranes were then fabricated using the solution casting method, a widely employed technique known for its consistency and reproducibility. The SPEEK solution was mixed with PIL (different types of PILs

Table 1
Physicochemical properties of used PILs.

Protic ionic liquids	Mol. Wt. (g/mol)	Viscosity @25 °C (cP)	σ (S cm^{-1}) (Temp. °C)
PIL1: 2-Hydroxyethylammonium formate	107.11	188	4.4×10^{-3} (25)
PIL2: Diethylmethylammonium triflate	237.24	37.7	8.1×10^{-3} (30)
PIL3: 1-Ethylimidazolium bis (trifluoromethylsulfonyl)imide	377.28	57.2	4.0×10^{-3} (30)
PIL4: 1,2-Dimethylimidazolium bis (trifluoromethylsulfonyl)imide	377.28	106	1.1×10^{-3} (25)
PIL5: Diethylmethylammonium methanesulfonate	183.27	111	6.2×10^{-3} (40)

and different loadings), stirred, and cast onto a clean glass petri dish. The membranes were dried at 60 °C for at least 24 h and further dried overnight under vacuum at 60 °C to remove any residual solvent. Table 2 shows the composition of the SPEEK-based composite PEMs.

2.2.2. FTIR spectroscopy

FTIR spectroscopy was employed to characterize the vibrational properties of all the PILs. FTIR spectra of the samples were acquired using a Perkin Elmer FTIR spectrophotometer (Spectrum 100, Perkin Elmer Cetus Instrument, Norwalk, CT, USA) in a KBr cell at room temperature, spanning the frequency range of 4000–400 cm⁻¹. Additionally, FTIR spectra of both neat SPEEK membrane and various SPEEK–PIL composite membrane samples were obtained in ATR mode at room temperature using a Nicolet iN10 FTIR (Thermo Scientific, Winsford, UK) equipped with a germanium microtip accessory, covering the frequency range of 4000–650 cm⁻¹.

2.2.3. Differential scanning calorimetry (DSC)

A differential scanning calorimeter, DSC 1 STAR^e System, Mettler Toledo AG, Analytical CH-8603 (Schwerzenbach, Switzerland) was used to analyze the behaviors of the pure SPEEK and SPEEK-PIL composites membranes. The samples were heated from room temperature to 120 °C at a heating rate of 10 °C per minute and held for 30 min to remove any moisture present in the sample then cooled to room temperature and then heated again to 300 °C to obtain the thermograms. The thermograms obtained in the second run were used for analysis. All the DSC measurements were made under a nitrogen environment.

2.2.4. Thermogravimetric analysis (TGA)

The thermal stability of the pure SPEEK and the SPEEK-PIL composites was investigated using a thermogravimetric analyzer, TGA/DSC 1 STAR^e System, Mettler Toledo AG, Analytical CH-8603, (Schwerzenbach, Switzerland) under an argon atmosphere with a flow rate of 50 mL/min. Samples weighing 8–10 mg were heated in alumina pans at a rate of 10 °C/min from room temperature to 650 °C. Additionally, the samples were held at 110 °C for 30 min to assess the moisture content of the membrane samples.

2.2.5. Electrochemical impedance spectroscopy (EIS)

Electrochemical impedance spectroscopy was employed to assess the ionic conductivity (σ) of the membranes. Stainless steel plates were used as blocking electrodes for the measurement (Gupta and Rhee, 2012). A K-type thermocouple was attached to the sample holder to monitor the exact temperature (T). The sample holder was kept in a small oven, which was controlled by a temperature controller. The measurement was carried out from 130 to 50 °C, starting the measurements from higher temperatures ensured the removal of any traces of moisture present in the samples and confirm that the reported ionic conductivity is for the anhydrous samples. A Palmsens4 Impedance Analyzer

Table 2
Composition details of the SPEEK-based composite PEMs.

Sample Name	SPEEK (wt.%)	PIL (wt.%)	PIL Used
SPEEK	100	0	–
SPIL1-45	55	45	2-Hydroxyethylammonium formate
SPIL2-35	65	35	Diethylmethylammonium triflate
SPIL2-45	55	45	Diethylmethylammonium triflate
SPIL2-55	45	55	Diethylmethylammonium triflate
SPIL2-65	35	65	Diethylmethylammonium triflate
SPIL2-75	25	75	Diethylmethylammonium triflate
SPIL3-45	55	45	1-Ethylimidazolium bis (trifluoromethylsulfonyl)imide
SPIL4-45	55	45	1,2-Dimethylimidazolium bis (trifluoromethylsulfonyl)imide
SPIL5-45	55	45	Diethylmethylammonium methanesulfonate

(PalmSens BV, Houten, The Netherlands) was employed to collect real and imaginary impedances across a frequency range spanning from 10⁵–1 Hz, with an alternating current amplitude of 20 mV. The bulk resistance (R_b) was determined from the high-frequency intercept of the Nyquist plot. The ionic conductivity was then calculated using the formula:

$$\sigma = l/(A R_b) \quad (1)$$

where l ($=0.04 \pm 0.01$ cm) represents the membrane thickness and A (≈ 0.785 cm²) denotes the area of the membrane.

3. Results and discussion

3.1. FTIR spectroscopy

FTIR spectrum of pure SPEEK membrane is shown in Figure S2 (Supplementary Information). The hydroxyl (–OH) groups are represented by a characteristic broad absorption band in the FTIR spectra, which appears around 3300–3500 cm⁻¹. Furthermore, the frequency ranges of 1050 cm⁻¹, 1250 cm⁻¹, and 1465 cm⁻¹ exhibit three distinct absorption bands of the –SO₃H groups. These absorption bands can be ascribed to the S = O stretching, the asymmetric O = S = O stretching, and the symmetric stretching vibration of O = S = O, respectively (Wu et al., 2019). The FTIR of various pure protic ionic liquids used in this

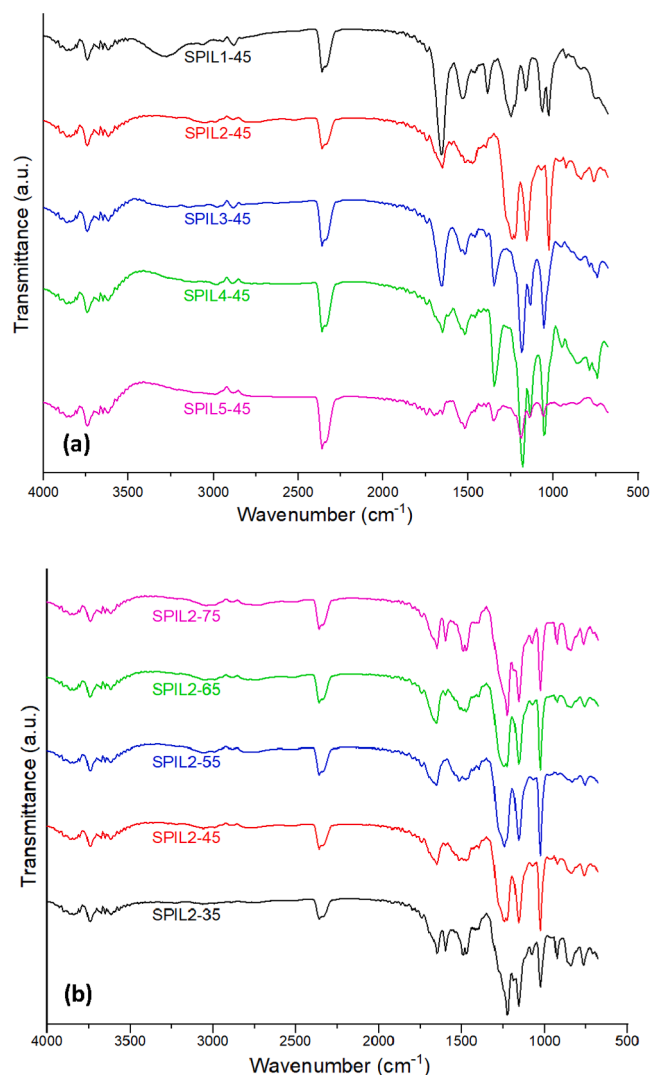


Fig. 1. FTIR spectra of the SPEEK-PIL composite membranes (a) with 45 wt% of PIL1–PIL5 and (b) 35–75 wt% of PIL2.

study along with their functional group analysis have been provided in (Figure S3-S7) supplementary information. In Fig. 1(a) the FTIR spectrum of the composite membrane SPIL1-45 shows free ionic formate groups appearing at 1530 cm^{-1} and 1382 cm^{-1} , which correspond to asymmetric and symmetric vibrations, respectively (Brownson et al., 2006). In the case of SPIL3-45 and PIL4-45, both contain bis(trifluoromethylsulfonyl)imide free ions, their FTIR spectra exhibit C = N stretching at around 1550 cm^{-1} for the aromatic groups of imidazolium ions. On the other hand, the bis(trifluoromethylsulfonyl)imide moiety display SO_2 asymmetric stretching, S-N-S asymmetric stretching and CF_3 symmetric bending at around 1348 cm^{-1} , 1053 cm^{-1} and 740 cm^{-1} , respectively (Park et al., 2022). In the diethylmethylammonium methanesulfonate protic ionic liquid-based composite (SPIL5-45), the small weak band at 740 cm^{-1} is due to S-C stretching, and 1056 cm^{-1} represents the symmetric SO_3 stretching vibration of the methanesulfonate moiety, which is well confirmed by previously reported literature (Pan et al., 2020). Also, there are some peaks that may have overlapped due to similar functional groups of SPEEK and PIL5.

The PIL2-based samples showed the highest proton conductivity among all other studied samples. Therefore, PEMs with different concentrations of PIL2 were prepared and tested, the FTIR analysis of these PEMs is presented in Fig. 1(b). The S = O symmetric stretching vibration frequency peak for the triflate ion is situated at 1030 cm^{-1} , while the peak around 1226 cm^{-1} could be assigned to the C - F stretching of the triflate ion (Mori et al., 2010; Yu et al., 2019). It is observed that as the overall concentration of triflate ions increases, the intensity of the above-mentioned band increases. It was observed that with an increase in the concentration of the PIL2 in the composites, the peak at 1465 cm^{-1} corresponding to the sulfonate groups increases due to an increase in the concentration of the sulfonate groups contributed by the PIL2 (Ali et al., 2019). The FTIR study suggests that all protic ionic liquids are well presented in the matrix and contribute to augmenting the proton conductivity of the fabricated composite membranes.

3.2. DSC analysis

The thermal transitions of both neat SPEEK and its different PIL-based composites are presented in Fig. 2(a) and the composites with different content of PIL2 (35–75 wt%) are illustrated in Fig. 2(b). In Fig. 2(a), it is evident that the neat SPEEK membrane exhibits a glass transition temperature (T_g) of $188\text{ }^\circ\text{C}$ at the midpoint, aligning with findings from previous studies (Akhtar et al., 2021; Banerjee and Kar, 2017; Jin et al., 1985; Zaidi et al., 2000). It further demonstrates that the addition of various PILs to the neat SPEEK polymer matrix results in a decrease in the glass transition temperatures of the composites compared to that of the neat SPEEK membrane. Notably, a singular glass transition temperature is discerned across all the composite membranes, signifying favorable compatibility between the ionic liquid and the SPEEK polymer matrix. In Fig. 2(b), however, a gradual and significant decrease in T_g is observed with the progressive incorporation of PIL2 into the SPEEK polymer matrix. This reduction could be attributed to a decrease in the intermolecular bonds of sulfonate groups within the SPEEK chain, induced by the introduction of the PILs (Yilmazoglu et al., 2021). The corresponding numerical values derived from their respective differential scanning calorimetry (DSC) thermograms are reported in Table 3.

3.3. TGA analysis

Fig. 3(a) and 3(b) show the TGA results for all the SPEEK-PIL composites with 45 wt% and SPEEK-PIL2 composites respectively, compared to the pure SPEEK matrix under inert atmospheres. To remove the moisture, all samples were held at $110\text{ }^\circ\text{C}$ for 30 min. The samples have amount of water ranging between 1 to 10 % by weight.

Fig. 3(a) shows a variation in the degradation behavior of the different PILs, however addition of any PIL results in a reduction of the

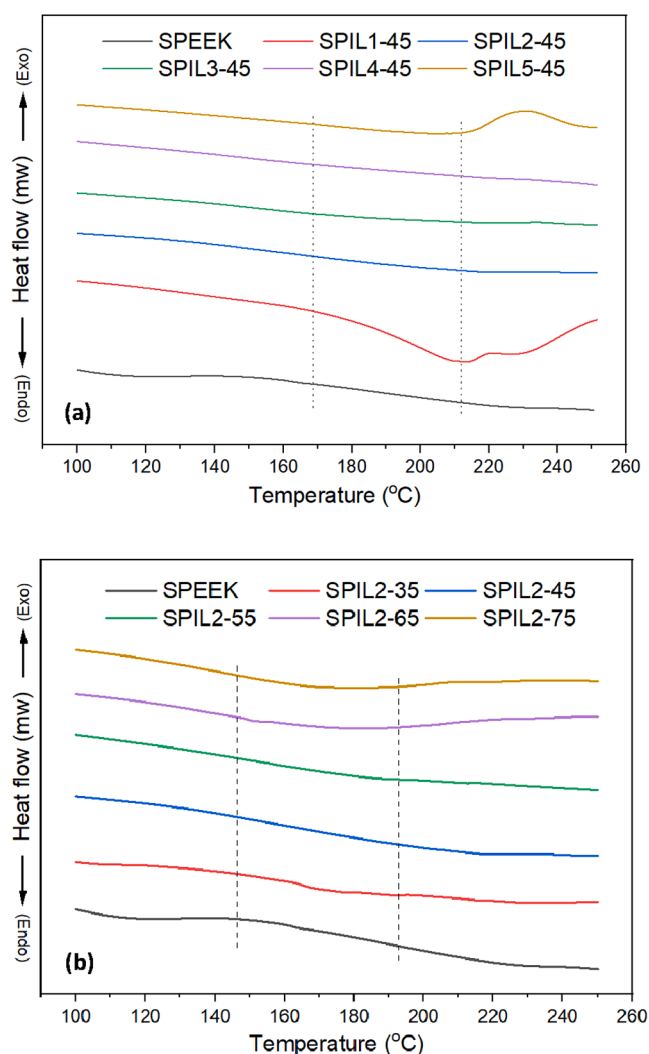


Fig. 2. DSC thermograms of the SPEEK-PIL composite membranes (a) with 45 wt% of PIL1-PIL5 and (b) 35–75 wt% of PIL2.

Table 3

Electrical transport properties and T_g values of the various composite PEMs.

Sample Name	$\sigma_{50^\circ\text{C}}$ (S cm^{-1})	$\sigma_{120^\circ\text{C}}$ (S cm^{-1})	E_a (eV)	T_g ($^\circ\text{C}$)
SPEEK	–	–	–	188
SPIL1-45	4.14×10^{-5}	4.86×10^{-4}	0.37	185
SPIL2-45	1.98×10^{-4}	2.27×10^{-3}	0.39	175
SPIL3-45	2.48×10^{-5}	8.60×10^{-4}	0.53	174
SPIL4-45	1.12×10^{-5}	5.65×10^{-4}	0.61	183
SPIL5-45	2.32×10^{-6}	1.30×10^{-4}	0.62	184
SPIL2-35	1.28×10^{-5}	5.02×10^{-4}	0.58	186
SPIL2-45	1.98×10^{-4}	2.27×10^{-3}	0.39	175
SPIL2-55	3.6×10^{-4}	3.36×10^{-3}	0.34	151
SPIL2-65	1.47×10^{-3}	8.04×10^{-3}	0.26	133
SPIL2-75	2.43×10^{-3}	8.33×10^{-3}	0.20	132

T_g – Glass transition temperature of SPEEK and its composite membranes as determined from the DSC thermograms.

thermal stability of the membrane. Although the thermal stability of the membranes has decreased, no significant weight loss due to degradation is observed up to around $170\text{ }^\circ\text{C}$, which makes these composites suitable for high-temperature applications.

As evident in Fig. 3(b), both the onset and end set of degradation of the SPEEK-PIL2 composites shift towards lower temperature with increasing PIL2 content compared to the neat SPEEK membrane. Moreover, incorporating the PIL into the SPEEK membrane structure

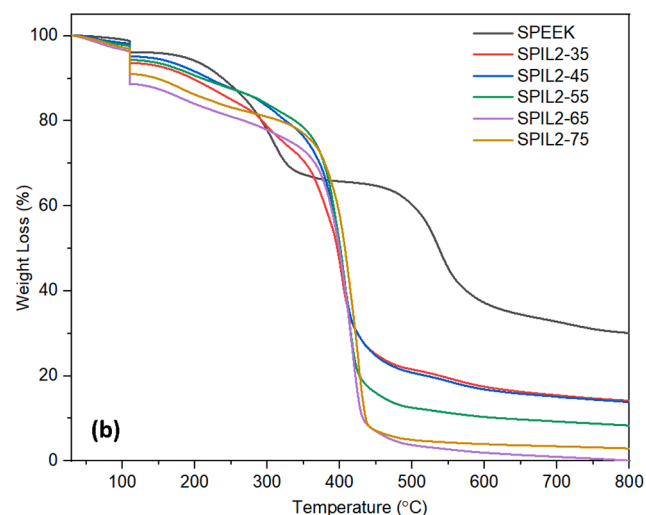
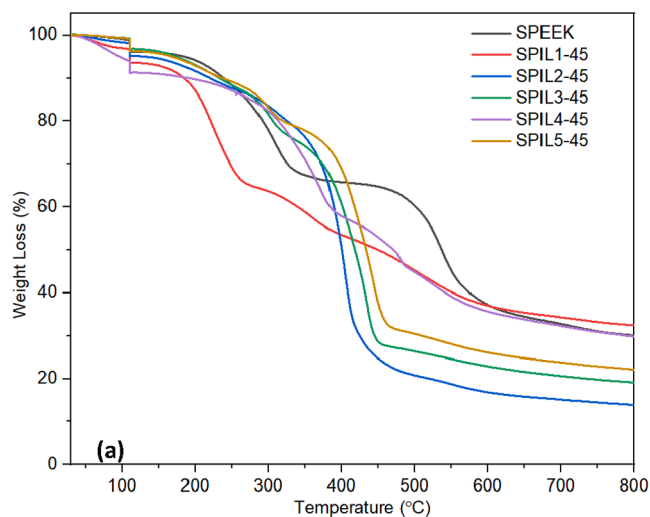


Fig. 3. TGA thermograms of the SPEEK-PIL composite membranes (a) with 45 wt% of PIL1-PIL5 and (b) 35–75 wt% of PIL2.

brought a different thermal behavior as the pure one exhibited a two-step decomposition pattern. The two steps observed in pure SPEEK membrane were attributed to the breakdown of the sulfonic acid group and the degradation of the main polymer backbone for the SPEEK membrane (Yilmazoglu et al., 2021).

3.4. XRD analysis

The effect of incorporation of the PIL on the crystallinity of SPEEK is evaluated by XRD. The XRD pattern of neat SPEEK and the SPEEK-PIL2 composite membranes are shown in Fig. 4. SPEEK membrane and its PIL2 composites exhibit characteristic XRD peaks at 2θ of 18.71° and 28.3° (Banerjee and Kar, 2017) (See Figure S8 in supplementary information for clear peak positions). The pure SPEEK membrane shows a wide peak at 2θ starting from 10° showing the amorphous phase of pure SPEEK membrane (Ali et al., 2019) and their composites. The characteristic peaks of the SPEEK-PIL2 composites are similar to those of pure SPEEK membrane. With an increase in the mass fraction of the PIL, a decrease in the intensity of the diffraction peaks is observed. This peak broadening is due to increase in amorphous region in the composites which can be attributed to structural changes in the ionic clusters, as they change from an ordered to disordered state due to their interaction with the incorporated PILs.

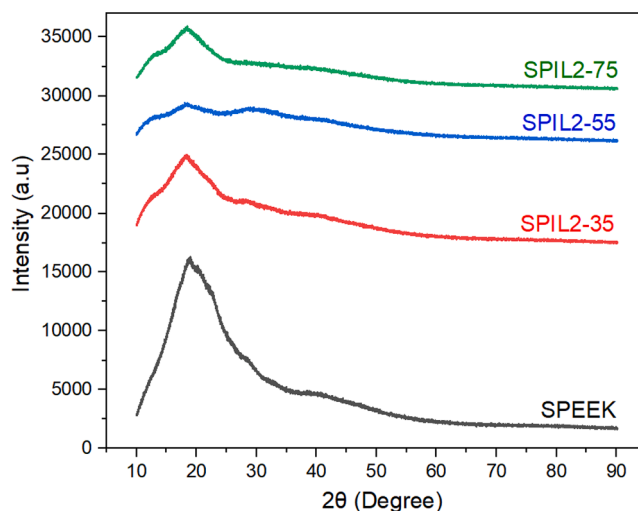


Fig. 4. XRD Pattern of Pure SPEEK and the composite membranes with various loadings of PIL2.

3.5. Electrical transport properties

As mentioned earlier, a fast ion-conducting electrolyte is needed for device applications. The requirement here is electrical conductivity (σ) greater than $10^{-3} \text{ S cm}^{-1}$ at 120°C for a high-temperature PEMFC. We recorded the real and imaginary parts of impedance (Z) for the composite electrolytes. Fig. 5 depicts the Nyquist curves of SPIL1-45 to SPIL5-45 at (a) 50°C and (b) 120°C . The Nyquist plots Fig. 5(a), at 50°C consisted of a semi-circle in the high-frequency zone (I) and nearly a straight line in the low-frequency zone (II) (Anis et al., 2023; Gupta et al., 2022). The semi-circle indicates the diffusion phenomenon of ions and the straight line portrays the blocking-electrode/polarization effect of the ions. These effects can be expressed by the equivalent circuit, $R_{s,I} + (R_b || C_1)_I + C_{2,II}$, where notations have their usual meaning (Careem et al., 2020). For example, R_s for a series resistance due to leads, R_b for bulk resistance, C_1 for chemical capacitance, and C_2 for double-layer capacitance. The subscripts I and II refer to high- and low-frequency zones, respectively. The existence of the semi-circle indicated that PIL molecules are physically attached to and homogeneously distributed in the SPEEK matrix. The level of completeness of the semi-circle suggests the ion-matrix interaction, which is the lowest for SPIL2-45 and the highest for SPIL5-45. The temperature significantly controls the ion-matrix interaction, as observed in Fig. 5(b), which indicates the Nyquist curves of SPIL1-45 to SPIL5-45 at $\approx 120^\circ\text{C}$. The semi-circle completely disappeared for the SPIL1-45 to SPIL4-45 samples at 120°C , suggesting a lower ion-matrix interaction because of the thermally activated phenomenon where the ions cooperate with the segmental motion of polymeric chains. The bulk resistance marked by an arrow at the intercept of the real axis was utilized to calculate the σ -value at ≈ 50 and 120°C (cf. Table 3). SPIL1-45, SPIL3-45, and SPIL4-45, having a partial semi-circle, exhibited $\sigma_{50^\circ\text{C}} \approx 10^{-5} \text{ S cm}^{-1}$. SPIL2-45, having a partial and small semi-circle, exhibited a higher value of $\sigma_{50^\circ\text{C}}$, $\approx 2 \times 10^{-4} \text{ S cm}^{-1}$. Whereas SPIL5-45, having a well-developed semi-circle, exhibited a low value of $\sigma_{50^\circ\text{C}}$, $\approx 2.3 \times 10^{-6} \text{ S cm}^{-1}$. At $\approx 120^\circ\text{C}$, SPIL1-45, SPIL3-45, SPIL4-45, and SPIL5-45 showed σ value more than $10^{-4} \text{ S cm}^{-1}$. Only SPIL2-45 possessed $\sigma_{120^\circ\text{C}} \approx 2.3 \times 10^{-3} \text{ S cm}^{-1}$, which is required for the device application (Agrawal and Gupta, 1999). Nakamoto and Watanabe (2007) extensively studied the various properties of several types of protic salts and concluded that the ionic liquid diethylmethylammonium trifluoromethanesulfonate is superior to other ionic liquids in many aspects. Lee et al. (2010) reported that diethylmethylammonium trifluoromethanesulfonate is preferable to diethylmethylammonium bis(trifluoromethane sulfonyl)imide in terms of fuel cell electrode reactions.

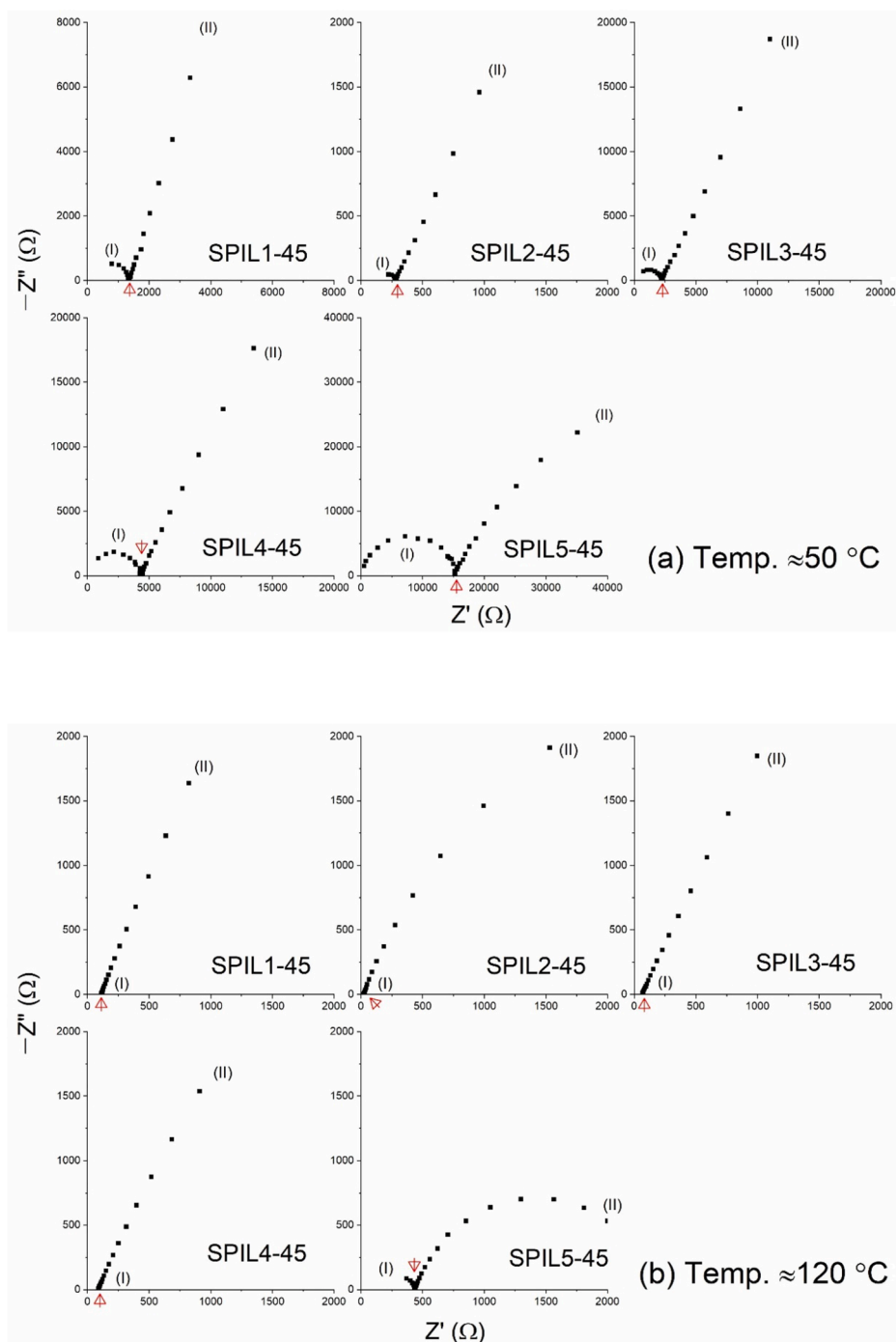


Fig. 5. Nyquist plot of the composite PEMs with 45 wt% loading of the different PILs (a) $\approx 50^\circ\text{C}$ and (b) $\approx 120^\circ\text{C}$.

The results of electrical conductivity contributed by the concentration and mobility of ions, can be explained in the light of the physico-chemical properties of the PILs (*cf.* Table 1). This is because the ionic mobility/conductivity is inversely proportional to the viscosity of the PILs (Singh et al., 2011). Additionally, an ion with a large size acts as a plasticizer to increase ionic mobility (Gupta et al., 2022). An anion with low lattice energy and donor number, and high molecular weight and dissociation constant is preferable for PIL dissociation in a polymer matrix (Gupta et al., 2024). A big size of the anion reduces its mobility and decreases its contribution to electrical conductivity. The formate ion had a size of 316 pm with a molecular weight of 107.11 g mol^{-1} and viscosity of 188 cP for PIL1, which produced SPIL1-45 with $\sigma_{50^\circ\text{C}} \approx 4.1 \times 10^{-5}\text{ S cm}^{-1}$. The bis(trifluoromethylsulfonyl)imide ion with a larger

ionic size, 790 pm, resulted in similar $\sigma_{50^\circ\text{C}}$ values, $2.5 \times 10^{-5}\text{ S cm}^{-1}$ for SPIL3-45 and $1.1 \times 10^{-5}\text{ S cm}^{-1}$ for SPIL4-45. SPIL3-45 had higher conductivity than SPIL4-45 because PIL3 had lower viscosity (57.7 cp) than PIL4 (106 cp). The triflate ion had lower ionic size (440 pm), molecular weight, and dissociation constant than the bis(trifluoromethyl sulfonyl)imide ion, however, with a similar level of dissociability, which resulted in the highest $\sigma_{50^\circ\text{C}}$ -value, $\approx 2 \times 10^{-4}\text{ S cm}^{-1}$ for SPIL2-45. This was most probably due to the lowest viscosity (37.7 cP) of PIL2. A replacement of F in triflate with H for methanesulfonate (ionic size 380 pm) produced PIL5, which had a lower molecular weight (183.27 g mol^{-1}) and a higher viscosity (111 cP). SPIL5-45, therefore, achieved the lowest $\sigma_{50^\circ\text{C}}$, $\approx 2.3 \times 10^{-6}\text{ S cm}^{-1}$. These findings are corroborative with the DSC study, discussed earlier.

A study on temperature-dependent σ -measurement reveals the nature of ion transport in the electrolyte. This study also provides activation energy (E_a), which should be less than 0.3 eV for the device application operating in a wide temperature range (Agrawal and Gupta, 1999). Fig. 6 exhibits a $\log \sigma$ vs. T^{-1} plot for SPIL1-45 to SPIL5-45. The composite PEMs showed a constant decrease in $\log \sigma$ with increasing T^{-1} , revealing the thermally activated phenomenon with the ions-cooperated segmental motion of the polymeric chains. The thermally activated linear curve ascertained the Arrhenius-type phenomenon with an equation, $\sigma = \sigma_0 \exp[-E_a/k_B T]$, where the notations σ_0 and k_B had their usual meanings. The linear fit provided the slope, thereby, the value of E_a for all the composite membranes, which are listed in Table 3. Only SPIL1-45 and SPIL2-45 possessed an E_a value less than 0.4 eV, close to the threshold for device application. However, we selected SPIL2-45 as the most suitable system because it had $\sigma_{120^\circ\text{C}}$ greater than 10^{-3} S cm^{-1} along with a favorable activation energy. We varied the PIL2 concentration to decrease the E_a value to less than 0.3 eV for the composite PEMs. Figure S9(a)(Supplementary Information) shows the Nyquist plot of SPIL2-35 to SPIL2-75 recorded at $\approx 50^\circ\text{C}$. These composite PEMs had a nearly complete high-frequency semi-circle for SPIL2-35, a partial and small semi-circle for SPIL2-45, and no semi-circle for SPIL2-55 to SPIL2-75. This trend in semi-circle suggests a decrease in ion-matrix interaction with increasing concentration of PIL2. The Nyquist plot of SPIL2-35 to SPIL2-75 recorded at $\approx 120^\circ\text{C}$ had no semi-circle Figure S9(b) (Supplementary Information). The intercept at the real axis of the impedance is marked by an arrow and corresponds to the bulk resistance. The bulk resistance values decreased with increasing concentration of PIL2. The σ -value at 50 and 120 $^\circ\text{C}$, computed from the bulk resistance, is listed in Table 3. The electrical conductivity@50 $^\circ\text{C}$ started from $\approx 1.3 \times 10^{-5}$ S cm^{-1} for SPIL2-35 and reached to $\approx 1.5 \times 10^{-4}$ S cm^{-1} for SPIL2-65. At 120 $^\circ\text{C}$, the σ -value started from $\approx 5 \times 10^{-4}$ S cm^{-1} for SPIL2-35 and reached to $\approx 8 \times 10^{-3}$ S cm^{-1} for SPIL2-65. No significant increase in the σ -value was noticed for SPIL2-75, revealing the saturation state. The increase in σ of the composite PEMs with increasing PIL content follows the expected trend. Pure PIL2 has $\sigma_{30^\circ\text{C}} \approx 8.1 \times 10^{-3}$ S cm^{-1} .

The temperature dependence of σ for the composite PEMs with different concentrations of PIL2 is depicted in Fig. 7. The PIL2 composites showed a linear decrease in $\log \sigma$ with increasing T^{-1} for all values the composite PEMs, revealing the Arrhenius-type phenomenon. An increase in σ with increasing temperature can be attributed to the enhanced mobility due to a reduction in the PIL at higher temperatures which in turn promotes the formation of interconnected anhydrous proton transfer channels. We computed the E_a values for all the PIL2-

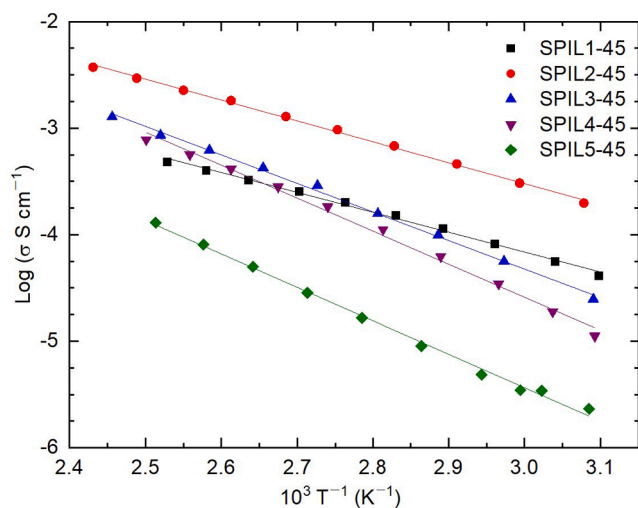


Fig. 6. Log σ - T^{-1} plot of composite PEM with 45 wt% loading of the different PILs.

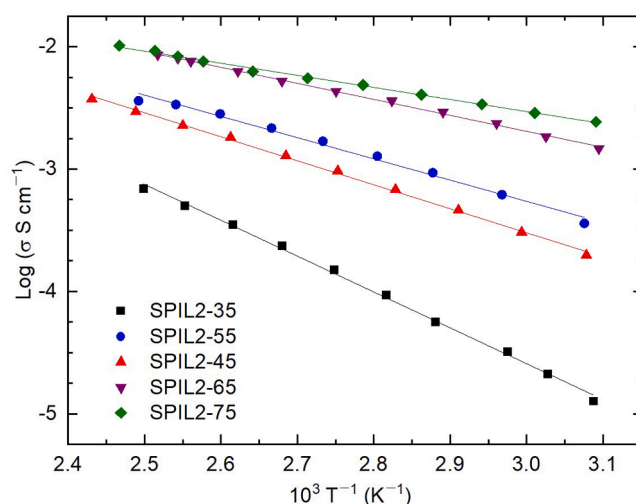


Fig. 7. Log σ - T^{-1} plot of the composite PEMs with different loadings of PIL2.

based composite PEMs and listed them in Table 3. This showed a decrease in E_a with increasing PIL2 concentration. SPIL2-65 achieved an impressive value of electrical transport parameters: $\sigma_{120^\circ\text{C}} \approx 8 \times 10^{-3}$ S cm^{-1} and $E_a \approx 0.26$ eV, making this a suitable candidate for PEMFC application.

4. Conclusions

SPEEK-PIL-based composite polymer electrolyte membranes were synthesized and characterized successfully to ascertain their thermal and physical properties for their suitability for applications in electrochemical devices. FTIR studies confirmed that no covalent bonds were formed between the PILs and the SPEEK sulfonic acid groups rather the interaction among them was purely ionic which helps to generate continuous proton transfer channels to improve the conductivity. The thermal properties of the composite PEMs were evaluated through DSC and TGA studies. The composite membranes showed the requisite thermal stability and the membranes were homogeneous and flexible due to the plasticizing effect of the incorporated PILs. The plasticizing effect of the PILs also led to a reduction in the glass transition temperatures of the composite membranes. The temperature dependence of proton conductivity of the SPEEK-PIL composite membranes was evaluated using EIS and was found to be in the order of 10^{-3} S cm^{-1} for the most of the composites at higher temperatures. The composite PEMs exhibited a linear $\log \sigma - T^{-1}$ curve, revealing the Arrhenius type of temperature-dependent behavior. The SPIL2-65 composite PEM achieved an impressive proton conductivity, $\approx 8 \times 10^{-3}$ S cm^{-1} at 120 $^\circ\text{C}$ and activation energy ≈ 0.26 eV, making this a suitable candidate for prospective PEMFC application.

Funding: This project was funded by the National Plan for Science, Technology and Innovation (MAARIFAH), King Abdulaziz City for Science and Technology, Kingdom of Saudi Arabia, Award Number (2-17-01-001-0042).

CRedit authorship contribution statement

Arfat Anis: Conceptualization, Data curation, Formal analysis, Funding acquisition, Investigation, Methodology, Project administration, Resources, Software, Supervision, Writing – original draft, Writing – review & editing. **Manawwer Alam:** Formal analysis, Investigation, Methodology, Writing – original draft. **Ravindra Kumar Gupta:** Data curation, Formal analysis, Investigation, Methodology, Software, Writing – original draft, Writing – review & editing. **Abdullah Alhamidi:** Data curation, Investigation, Methodology. **Hamid Shaikh:** Conceptualization, Investigation, Writing – original draft, Writing –

review & editing. **Anesh Manjaly Poulouse**: Formal analysis, Investigation, Writing – review & editing. **Mohammad Asif Alam**: Investigation, Writing – original draft, Writing – review & editing. **Saeed M. Al-Zahrani**: Conceptualization, Project administration, Resources, Supervision, Writing – review & editing.

Declaration of Competing Interest

The authors declare that they have no known competing financial interests or personal relationships that could have appeared to influence the work reported in this paper.

Appendix A. Supplementary data

Supplementary data to this article can be found online at <https://doi.org/10.1016/j.jksus.2024.103215>.

References

- Agrawal, R.C., Gupta, R.K., 1999. Superionic solids: Composite electrolyte phase - an overview. *Journal of Materials Science* 34, 1131–1162.
- Akhtar, F.H., Abdulhamid, M.A., Vovusha, H., Ng, K.C., Schwingschlögl, U., Szekeley, G., 2021. Defining sulfonation limits of poly (ether-ether-ketone) for energy-efficient dehumidification. *Journal of Materials Chemistry A* 9, 17740–17748.
- Ali, M.M., Rizvi, S.J.A., Azam, A., 2019. Fabrication of proton exchange membranes and effect of sulfonated sio2 (s-sio2) in sulfonated polyether ether ketone (speek) for fuel cells applications. *IOP Conference Series: Materials Science and Engineering* 577, 012039.
- Anis, A., Alam, M., Alhamidi, A., Gupta, R.K., Tariq, M., Al-Zahrani, S.M., 2023. Studies on polybenzimidazole and methanesulfonate protic-ionic-liquids-based composite polymer electrolyte membranes. *Polymers* 15 (13), 2821.
- Banerjee, S., Kar, K.K., 2017. Impact of degree of sulfonation on microstructure, thermal, thermomechanical and physicochemical properties of sulfonated poly ether ether ketone. *Polymer* 109, 176–186.
- Brownson, J.R., Tejedor-Tejedor, M.I., Anderson, M.A., 2006. Ftir spectroscopy of alcohol and formate interactions with mesoporous tio2 surfaces. *The Journal of Physical Chemistry B* 110, 12494–12499.
- Cappadonia, M., Niemzig, O., Stimming, U., 1999. Preliminary study on the ionic conductivity of a polyphosphate composite. *Solid State Ionics* 125, 333–337.
- Careem, M.A.; Noor, I.S.M.; Arof, A.K. Impedance spectroscopy in polymer electrolyte characterization. In *Polymer electrolytes*, Winie, T.; Arof, A.K.; Thomas, S., Eds. 2020; pp 23-64.
- Devanathan, R., 2008. Recent developments in proton exchange membranes for fuel cells. *Energy & Environmental Science* 1, 101–119.
- Eguizábal, A., Lemus, J., Pina, M., 2013. On the incorporation of protic ionic liquids imbibed in large pore zeolites to polybenzimidazole membranes for high temperature proton exchange membrane fuel cells. *Journal of Power Sources* 222, 483–492.
- Gupta, R.K., Rhee, H.W., 2012. Effect of succinonitrile on electrical, structural, optical, and thermal properties of poly(ethylene oxide)-succinonitrile /lii-i-2 redox-couple solid polymer electrolyte. *Electrochimica Acta* 76, 159–164.
- Gupta, R.K., Shaikh, H., Imran, A., Bedja, I., Ajaj, A.F., Aldwayyan, A.S., 2022. Electrical transport, structural, optical and thermal properties of [(1-x)succinonitrile: Xpeo]-litfsi-co(bpy)3(tfsi)2-co(bpy)3(tfsi)3 solid redox mediators. *Polymers* 14 (9), 1870.
- Gupta, R.K., Shaikh, H., Imran, A., Bedja, I., Ajaj, A.F., Aldwayyan, A.S., Khan, A., Ayub, R., 2024. Electrical transport properties of (1-x)succinonitrile: X poly (ethylene oxide) -licf3so3 -co tris-(2,2'-bipyridine)3(tfsi)2-co tris-(2,2'-bipyridine)3 (tfsi)3 solid redox mediators. *Rsc Advances* 14, 539–547.
- Jin, X., Bishop, M.T., Ellis, T.S., Karasz, F.E., 1985. A sulphonated poly (aryl ether ketone). *British Polymer Journal* 17, 4–10.
- Johnson, L., Ejigu, A., Licence, P., Walsh, D.A., 2012. Hydrogen oxidation and oxygen reduction at platinum in protic ionic liquids. *The Journal of Physical Chemistry C* 116, 18048–18056.
- Lee, S.-Y., Yasuda, T., Watanabe, M., 2010. Fabrication of protic ionic liquid/sulfonated polyimide composite membranes for non-humidified fuel cells. *Journal of Power Sources* 195, 5909–5914.
- Maiti, T.K., Dixit, P., Singh, J., Talapatra, N., Ray, M., Chattopadhyay, S., 2023. A novel strategy toward the advancement of proton exchange membranes through the incorporation of propylsulfonic acid-functionalized graphene oxide in crosslinked acid-base polymer blends. *International Journal of Hydrogen Energy* 48 (4), 1482–1500.
- Mori, K., Hashimoto, S., Yuzuri, T., Sakakibara, K., 2010. Structural and spectroscopic characteristics of a proton-conductive ionic liquid diethylmethylammonium trifluoromethanesulfonate [dema][tfoh]. *Bulletin of the Chemical Society of Japan* 83, 328–334.
- Nakamoto, H., Watanabe, M., 2007. Brønsted acid–base ionic liquids for fuel cell electrolytes. *Chemical Communications* 2539–2541.
- Pan, H., Geysens, P., Putzeys, T., Gennaro, A., Yi, Y., Li, H., Atkin, R., Binnemans, K., Luo, J., Wübbenhorst, M., 2020. Physicochemical study of diethylmethylammonium methanesulfonate under anhydrous conditions. *The Journal of Chemical Physics* 152, 234504.
- Park, S., Kim, B., Cho, C., Kim, E., 2022. Mesogenic polymer composites for temperature-programmable thermoelectric ionogels. *Journal of Materials Chemistry A* 10, 13958–13968.
- Quartarone, E., Mustarelli, P., 2012. Polymer fuel cells based on polybenzimidazole/h 3 po 4. *Energy & Environmental Science* 5, 6436–6444.
- Singh, P.K., Nagarale, R.K., Pandey, S.P., Rhee, H.W., Bhattacharya, B., 2011. Present status of solid state photoelectrochemical solar cells and dye sensitized solar cells using peo-based polymer electrolytes. *Advances in Natural Sciences: Nanoscience and Nanotechnology* 2, 023002.
- Sun, L., Qu, S., Lv, X., Duan, J., Wang, W., 2023. *J. Appl. Polym. Sci.* 140 (4), e53384.
- Wang, X., Jin, M., Li, Y., Zhao, L., 2017. The influence of various ionic liquids on the properties of speak membrane doped with mesoporous silica. *Electrochimica Acta* 257, 290–300.
- Wang, J., Yue, Z., Economy, J., 2007. Preparation of proton-conducting composite membranes from sulfonated poly (ether ether ketone) and polyacrylonitrile. *Journal of Membrane Science* 291, 210–219.
- Wu, G., Lin, S.-J., Hsu, I.-C., Su, J.-Y., Chen, D.W., 2019. Study of high performance sulfonated polyether ether ketone composite electrolyte membranes. *Polymers* 11, 1177.
- Xiong, C., Ling, Z., Wang, B., Yu, Y., Liu, Q., Fu, X., Wu, C., Zhang, R., Hu, S., Bao, X., Yang, J., 2024. Electrospinning-assisted construction of rapid proton conduction channels in halloysite nanotube-encapsulated ionic liquid-embedded sulfonated poly (ether ether ketone) proton exchange membranes. *Fuel* 362, 130814.
- Yılmazoğlu, M., Bayiroğlu, F., Erdemi, H., Abacı, U., Guney, H.Y., 2021. Dielectric properties of sulfonated poly (ether ether ketone)(speek) electrolytes with 1-ethyl-3-methylimidazolium tetrafluoroborate salt: Ionic liquid-based conduction pathways. *Colloids and Surfaces a: Physicochemical and Engineering Aspects* 611, 125825.
- Yılmazoğlu, M., Bayiroğlu, F., Erdemi, H., Abacı, U., Guney, H.Y., 2023. Ionic liquid incorporated SPEEK/Chitosan solid polymer electrolytes: ionic conductivity and dielectric study. *J Solid State Electrochem* 27, 1143–1154.
- Yu, J., Kikuchi, S., Peediyakkal, H.P., Munakata, H., Kanamura, K., 2019. Phosphoric acid diethylmethylammonium trifluoromethanesulfonate-based electrolytes for nonhumidified intermediate temperature fuel cells. *ACS Applied Materials & Interfaces* 11, 13761–13767.
- Zaidi, S., Mikhailenko, S.D., Robertson, G., Guiver, M., Kaliaguine, S., 2000. Proton conducting composite membranes from polyether ether ketone and heteropolyacids for fuel cell applications. *Journal of Membrane Science* 173, 17–34.
- Zhang, H., Shen, P.K., 2012. Recent development of polymer electrolyte membranes for fuel cells. *Chemical Reviews* 112, 2780–2832.